International Journal of Civil Engineering

Geotechnical Engineering

Investigation of foundations behavior by implementation of a developed constitutive soil model in the ZEL method

M. Jahanandish[1,*], M. Veiskarami[2], A. Ghahramani[3]

Received: May 2010, Accepted: January 2011

Abstract

Foundations behavior is affected by soil behavior which can vary from dilative to contractive depending on the stress level, particularly in dense frictional soils. The Zero Extension Lines (ZEL) method has been generally developed to predict the foundations behavior. Knowledge of soil behavior enables the ZEL method to predict the general and local shear failure modes. In this paper, a relatively simple work hardening/softening soil constitutive model is developed to represent dense frictional soils behavior under different stress levels. This model is based on the accumulation of the plastic work during a simple direct shear test and its relationship to stress ratio to establish the hardening law. Verifications have been made for the developed soil model. The model is then implemented into the ZEL method to theoretically investigate the bearing capacity and load-displacement behavior of foundations over dense frictional soils. Utilization of this model enables the ZEL method to capture different modes of failure depending on the foundation size. A numerical study on foundations behavior was performed showing the ability of the presented approach in capturing both failure modes.

Keywords: Constitutive soil model, Plasticity, Foundation, Stress level, ZEL

1. Introduction

There is a long history on determination of the bearing capacity of shallow foundations. Several theoretical and experimental methods to determine actual bearing capacity of shallow foundations have been developed in the past decades [1,2]. The famous triple-N formula of Karl Terzaghi in 1943 that has been widely accepted by researchers is as follows [1,2]:

$$q_{ult} = cN_c + qN_q + 0.5\gamma BN_\gamma \quad (1)$$

In this equation, q_{ult} is ultimate bearing capacity, c is cohesion, q is the surcharge pressure, B is the foundation width (or diameter), γ is soil density and N_i coefficients are the bearing capacity factors defined as functions of soil friction angle, ϕ.

For shallow foundations over cohesionless soils, the third factor is the main bearing capacity contributor. Numerous methods, based on limit theorems, have been developed in determination of the bearing capacity of shallow foundations, in particular for the bearing capacity factor N_γ [1-11]. In most of these methods a plastic region of soil is supposed to form beneath the foundation at the ultimate bearing capacity. This ultimate load satisfying the equilibrium-yield conditions can be found by plasticity theory. Although the third term in the bearing capacity equation suggests a linear increase in the bearing capacity with foundation width or diameter, experimental observations of De Beer (1965) and Ovesen (1975), and other researchers, shows a different behavior [12,13]. A decreasing tendency in the ultimate bearing capacity of shallow foundations was widely observed and reported in small scale, full scale and centrifuge tests [14-19]. Lately, Kumar and Khatri (2008) performed an experimental foundation load test along with a numerical study on the bearing capacity of shallow foundations and stated that the bearing capacity factor, N_γ, decreases almost linearly with foundation size on a log-log scale plot [20].

Most of the aforementioned attempts have mainly focused on determination of the ultimate bearing capacity of foundations. It should be noted that the ultimate bearing capacity is also deduced from the failure mechanism which may vary from a general shear failure for a relatively dense soil to a local shear failure for a loose soil [2,5,16] and hence,

* *Corresponding Author: jahanand@shirazu.ac.ir*
1 Associate Professor, Dept. of Civil Eng., Shiraz University, Shiraz, Iran
2 Ph.D. Candidate in Geomechanics, Shiraz University, Shiraz, Iran
3 Professor, Dept. of Civil Eng., Shiraz University, Shiraz, Iran

foundations behavior can be predicted when the subsoil behavior is well understood. To do this and for many more applications in soil mechanics by principles of soil plasticity, a great number of constitutive soil models have been developed and applied in the literature (Poorooshasb et al., 1966; Poorooshasb et al., 1967; Lade and Duncan, 1975; Nova and Wood, 1979; Hamidi et al., 2009; Sadrnejad *et al*, 2010) [21-27]. Most of these models comprise many parameters which are rather difficult to be determined by conventional laboratory tests. Application of constitutive models in the theoretical prediction of foundations behavior and numerical modeling of shallow and deep foundations have been well reported in the literature [28,29].

Very recently, Yamamoto *et al*. (2009) performed a numerical analysis on the bearing capacity and load-displacement behavior of shallow foundation on two different sands [30]. Their work was mainly focused on utilizing the MIT-S1soil model into the ABAQUS finite element code for the numerical analyses [30,31]. This soil model comprises of 13 parameters that may be obtained from extensive experimental tests [30-33].

Roscoe (1970) introduced the role of strains in problems dealing with soil and introduced the Zero Extension Lines (ZEL) directions along which linear strain increments are zero [34]. This concept is a useful method in particular for load-displacement prediction of structures in contact with soil. This concept was later employed by James and Bransby (1971) to determine strain and displacement patterns behind model retaining walls [35]. Habibagahi and Ghahramani (1979) and Ghahramani and Clemence (1980) calculated the soil pressures by considering the force-equilibrium of soil elements between the zero extension lines [36,37]. The methodology for finding the load-deflection behavior of foundation and retaining walls on the basis of the ZEL theory was presented by Jahanandish *et al*. (1989) [38]. The general form of these lines were considered in this methodology and the variations of soil strength parameters c and ϕ, with the induced shear strain due to the deflection of the structure were also taken into account. In 1997, Anvar and Ghahramani used the matrix method for derivation of differential equilibrium-yield equations along the stress characteristics in plane strain condition, and transferred them along the Zero Extension Lines [39]. This approach was important since it allowed integration of the equations along the zero extension directions. In 2003, Jahanandish considered the more general case of axial symmetry, and obtained the equilibrium-yield equations along the Zero Extension Lines by direct transformation, independent from the stress characteristics [40]. Details of these derivations can be found in Anvar and Ghahramani 1997) [39] and Jahanandish (2003) [40]. Development of the zero extension line method for the more general three dimensional case has also been made recently by Jahanandish et. al. (2010) [41].

In this research, the ability of the ZEL method is utilized to predict foundations behavior on frictional soils. General shear failure mechanisms, with apparent peak strength, and local shear failure mechanisms without a peak, are expected to be predictable by this method. In order to find the load-displacement curves, the relationship between soil mobilized friction angle and soil maximum shear strain is required for the ZEL method. Regarding the difficulties in performing triaxial tests on sand and the difficulties in determination of the model parameters for existing constitutive soil models found in the literature, a simple work hardening/softening constitutive soil model has been developed in this research based on direct shear tests results which is a conventional test for cohesionless soils. This model is capable of predicting both dilative and contractive soil behaviors from direct shear tests performed at different stress levels. This model is then incorporated into a developed computer code to analyze the load-displacement behavior of shallow foundations. A numerical study is then performed to show the ability of the model in distinguishing different foundation behaviors resulted from different failure mechanisms.

2. Plasticity Equations along the Zero Extension Lines

The ZEL method concerns with solution of plasticity equations, i.e. equilibrium and yield equations, along the ZEL direction. Using Mohr-Coulomb yield criterion and defining angle ψ to be the angle between maximum principal stress direction and horizontal direction as illustrated in Fig. 1a, the zero extension directions are defined by [39,40]:

Equations for the ZEL Directions:

$$\begin{cases} \text{For +tive direction:} \dfrac{dz}{dr} = \tan(\psi + \xi) \\ \text{For -tive direction:} \dfrac{dz}{dr} = \tan(\psi - \xi) \end{cases} \quad \text{and} \quad \xi = \frac{\pi}{4} - \frac{\nu}{2} \tag{2}$$

Where $\xi=\pi/4-\nu/2$, and the minus sign (-), stands for the one direction and the plus sign (+), for the other which are shown in Fig. 1b, on a Mohr's circle of strain. Fig. 1c shows the ZEL directions and stress characteristics for an arbitrary soil element. Based on Anvar & Ghahramani's (1997) derivation, the equilibrium-yield equations along the Zero Extension Lines for the plane strain problem are as follows [39]:

Anvar and Ghahramani (1997) Equations along the ZEL Directions:

$$\begin{cases} \text{Along the minus (-) ZEL:} \\ dS - 2(S\tan\phi + c)\left(\bar{\alpha}\, d\theta + \bar{\zeta}\dfrac{\partial\psi}{\partial\varepsilon^+} d\varepsilon^-\right) = X\bar{\beta}(\tan\phi\, dz + \bar{\alpha}\, dx) - Z\bar{\beta}(\tan\phi\, dx - \bar{\alpha}\, dz) \\ +(S - c\tan\phi)\left(\tan\phi\, d\phi - \dfrac{1}{\cos\phi}\dfrac{\partial\phi}{\partial\varepsilon^+} d\varepsilon^-\right) + \left(\tan\phi\, dc - \dfrac{1}{\cos\phi}\dfrac{\partial c}{\partial\varepsilon^+} d\varepsilon^-\right) \\ \text{Along the plus (+) ZEL:} \\ dS + 2(S\tan\phi + c)\left(\bar{\alpha}\, d\theta + \bar{\zeta}\dfrac{\partial\psi}{\partial\varepsilon^-} d\varepsilon^+\right) = -X\bar{\beta}(\tan\phi\, dz - \bar{\alpha}\, dx) + Z\bar{\beta}(\tan\phi\, dx + \bar{\alpha}\, dz) \\ +(S - c\tan\phi)\left(\tan\phi\, d\phi - \dfrac{1}{\cos\phi}\dfrac{\partial\phi}{\partial\varepsilon^-} d\varepsilon^+\right) + \left(\tan\phi\, dc - \dfrac{1}{\cos\phi}\dfrac{\partial c}{\partial\varepsilon^-} d\varepsilon^+\right) \end{cases} \tag{3}$$

In these equations, X and Z are the body and/or inertial forces along x and z directions and $d\varepsilon^+$ and $d\varepsilon^-$ are length of the differential elements along the ZEL directions. The values of $\bar{\alpha}$, $\bar{\beta}$ and $\bar{\zeta}$ are given by:

$$\bar{\alpha} = \frac{1 - \sin\phi\sin\nu}{\cos\phi\cos\nu}, \quad \bar{\beta} = \frac{\cos\nu}{\cos\phi}, \quad \bar{\zeta} = \frac{\sin\phi - \sin\nu}{\cos\phi\cos\nu} \tag{4}$$

Based on Jahanandish (2003) derivation, the final form of equilibrium-yield equations along the ZEL directions for the more general case of axial symmetry is [40]:

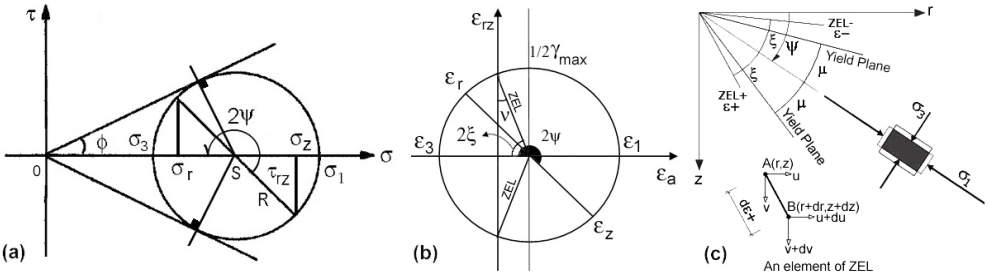

Fig. 1. Mohr circles of stress and strain: a) Minor and major principal stresses and b) Minor and major principal strains with ZEL directions and c) Directions of stress characteristics and the Zero Extension Lines

Jahanandish (2003) Equations along the ZEL Directions:

$$\begin{cases} \text{Along the minus (-) ZEL:} \\ dS+\dfrac{\partial T}{\partial \varepsilon^+}d\varepsilon^- -\dfrac{2T}{\cos\nu}(d\psi-\sin\nu\dfrac{\partial \psi}{\partial \varepsilon^+}d\varepsilon^-)=[f_r\cos(\psi-\xi)+f_z\sin(\psi-\xi)]d\varepsilon^- \\ \text{Along the plus (+) ZEL:} \\ dS+\dfrac{\partial T}{\partial \varepsilon^-}d\varepsilon^+ +\dfrac{2T}{\cos\nu}(d\psi-\sin\nu\dfrac{\partial \psi}{\partial \varepsilon^-}d\varepsilon^+)=[f_r\cos(\psi+\xi)+f_z\sin(\psi+\xi)]d\varepsilon^+ \end{cases} \quad (5a)$$

In these equations, T is the radius of Mohr circle for stress, and n is an integer equal to 1 for the axi-symmetric problems and 0 for the plane strain case. f_r and f_z are expressed by:

$$\begin{cases} f_r = X-\dfrac{n}{r}(\sigma_r-\sigma_\theta) \\ f_z = Z-\dfrac{n}{r}\tau_{rz} \end{cases} \quad \sigma_\theta=\sigma_3 \Rightarrow \begin{cases} f_r = X-\dfrac{nT}{r}(1+\cos 2\psi) \\ f_z = Z-\dfrac{nT}{r}\sin 2\psi \end{cases} \quad (5b)$$

As mentioned; these equations are more general so that those for plane strain can simply be deduced from them by setting n=0 and $T=S\sin\phi+C\cos\phi$. Note that r is the measure of the radial distance for the axi-symmetric problem.

Since the Zero Extension Lines work as rigid links between their start and end nodes, the displacement of any ZEL segment should be normal to this segment and therefore, the following expression is resulted [39,40]:

$$\frac{du}{dv}=-\frac{dz}{dr} \quad (6)$$

In this equation, u and v are lateral and vertical displacement increments along r and z respectively. These equations can be written in a finite difference form and if a displacement boundary is known, the strain and displacement fields can be found. It should also be mentioned that the variation in soil strength parameters c and ϕ has also been considered in the ZEL equations. Variation in c and ϕ can be due to non-homogeneity of the soil mass. It can also be due to the difference in shear stain at different points of the soil. This later relation has already been used in obtaining the load-deflection behavior of structures in contact with soil [36-40]. It requires the relationship between soil maximum shear strain and $\sin\phi_{mob}$. In this research a constitutive soil model has been implemented in the ZEL method describing soil behavior under different stress levels. The ZEL equations can be solved by numerical techniques in a triple point strategy. Details of such solution technique has been described by Anvar and Ghahramani (1997) and Jahanandish, (2003) [39,40].

Computation of the Deformations

The main property of the ZEL net can be employed to find the velocity field and for a given deformation boundary condition, the generated displacements in the ZEL net can be computed using the finite difference form of Eq. 6 for any two successive points. For example a rotating boundary is shown in Fig. 2. The left boundary is held fixed against translation. To find the final position of point, say, B_2 after deformation it is sufficient to rewrite Eq. 6 in a finite difference form. Knowing the displacements of points A_2 and A_3, the displacements of point B_2, i.e., uB_2 and vB_2 will be obtained [39,40]. Appendix A represents a summary of the solution technique of these equations.

3. Developed Constitutive Soil Model

The developed constitutive soil model in this work is expected to be a simple model conforming to the requirements of the ZEL method. In this model the mobilized shear strain is related to the mobilized shear strength which can then be easily converted to the mobilized friction angle, ϕ_{mob}., required by the ZEL method. This model is primarily based on the direct shear tests results which are common for most of granular soils, regarding difficulties involved in performing triaxial tests on such materials. One of the basic concepts behind this model is the hypothesis presented by Wood (1990) and Atkinson (2008), in which, soil behavior is related to the angle of dilatation [42,43]. The framework of Lade and Duncan (1975) in developing a hyperbolic work hardening constitutive soil model for sand is also considered and followed in this work [24].

Simple Shear and Dilation Model

Fig. 3a shows the simple shearing and dilation model of a

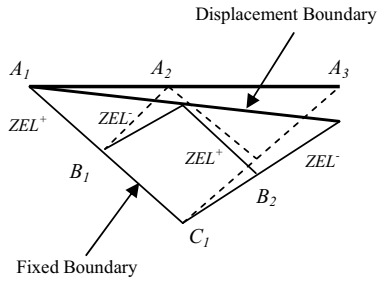

Fig. 2. A schematic deformed ZEL net

sliding object over an inclined rough surface which is presented by several authors (Wood, 1990; Atkinson, 2008) [42,43]. Required shear force to overcome the net mobilized horizontal forces, due to surface roughness and due to inclination depends on surface coefficient of roughness and inclination. This force may be equal to, more or less than the frictional force resulting only from the roughness of the surface. Fig. 3b shows the application of this model for dense soils in a direct shear test with resulting soil behavior depicted in Fig. 3c. According to this hypothesis, the mobilized soil friction angle, $\phi_{mob.}$, can be considered as a resultant of critical state friction angle, $\phi_{c.s.}$, in which no volume change occurs during further deformation, and soil angle of dilation, υ, describing the dilatational tendency of soil when it is sheared.

Accordingly, the following definitions could be made:

$$\nu = \tan^{-1}(\frac{\delta v}{\delta h}) \tag{7a}$$

$$\phi_{mob.} = \mu + i = \phi_{c.s.} + \nu \tag{7b}$$

$$\frac{T}{N} = \tan\phi_{mob.} = \tan(\phi_{c.s.} + \nu) \tag{7c}$$

In these equations, υ is soil angle of dilation which is equivalent to the inclination, i, of the sliding surface, δv and δh are vertical and horizontal displacement increments, $\phi_{c.s.}$ is the critical state friction angle which is mobilized when there is no further volume change (no dilation and no contraction) and it corresponds to the intrinsic surface friction, μ, in a case of horizontal surface (with no inclination) in the previous hypothesis, N is the normal force and T is the shear force acting on the sliding surface.

The major fact is that although $\phi_{c.s.}$ is a constant material parameter, v is a state dependent parameter that varies with shear strain and stress level and hence, mobilized soil friction angle varies during a shear test on a frictional soil [42,43]. Therefore, absolute value of soil mobilized friction angle can be considered to be the sum of soil critical state friction angle, $\phi_{c.s.}$ which is a constant value and soil dilation angle which varies during soil shearing. It has been also well observed and reported in the literature that soil behavior is stress level dependent and a dense soil may demonstrate a loose soil (contractive) behavior when tested at sufficiently high stress levels (Meyerhof, 1950; DeBeer, 1965; Lee and Seed, 1967; Bolton, 1986; Gan et al., 1988; Maeda and Miura, 1999; Budhu, 2007; Kumar et al., 2007) [44-51]. As a result, a dilatational behavior is expected under relatively low stresses whereas a contractive behavior may be observed under relatively high stresses for a certain soil type in both triaxial and direct shear tests.

In order to describe the behavior of foundations over a dense soil with stress level dependency consideration, an attempt should be made to derive a constitutive relationship linking plastic strain to the current stress state. Therefore, it is necessary to develop a corresponding constitutive soil model capable of capturing the actual dilative or contractive soil behavior under different stress level states. This model can then be utilized in an appropriate analytical code, which is the ZEL method in this study.

Requirements of the Constitutive Soil Model

Regarding soil plasticity theories, the total strain in a soil element is the sum of the elastic and plastic parts:

$$\varepsilon_{ij} = \varepsilon_{ij}^{e} + \varepsilon_{ij}^{p} \tag{8}$$

in which, the superscripts *e* and *p* indicate elastic and plastic strains. While the elastic strains can be computed by the use of elasticity theories, the plastic strains are relatively difficult to be determined. It is conventional to consider the *incremental strains* rather than the *total strain*s. Despite this obvious fact that the plastic strains may possibly become quite large, the small-strain definitions are used. Most of engineering materials can exhibit increase in strength beyond the elastic limits. This phenomenon is called hardening, whereas this behavior is called softening when materials show a decrease in strength during progressive straining after the peak strength is reached. As a consequence, for a complete elasto-plastic constitutive model, it is necessary to include the following parts (Lade and Duncan, 1975) [24]:

- Elasticity parameters and relationships to find elastic strains.
- A yield criterion such that if the soil is subjected to change in stress presented by points inside the yield surface, the soil deforms elastically, whereas if the changes in stress tend to cross the yield surface it will simultaneously yield plastically and deform elastically.

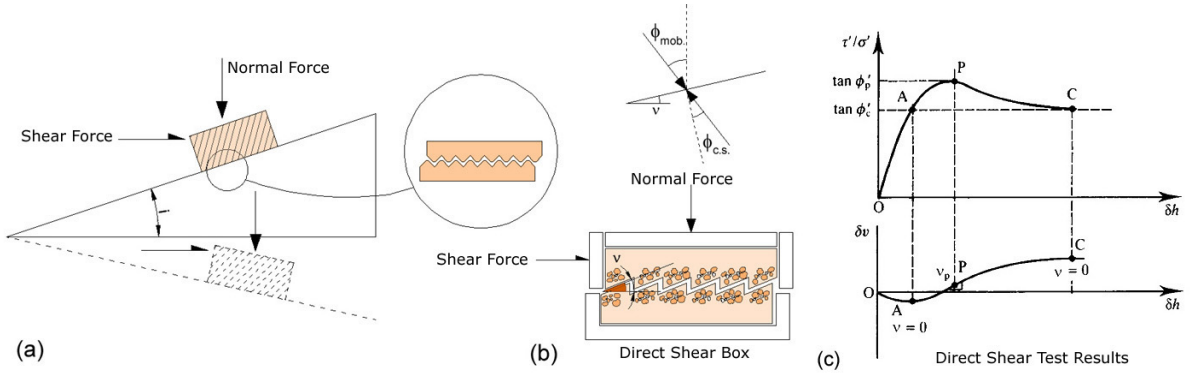

Fig. 3. Application of the sliding on inclined rough surface model a) Inclined rough surface with frictional irregularities, b) direct shear box and mobilized friction angle and c) direct shear test results

• A flow rule and plastic potential function which relate the relative magnitudes of the strain increments to stresses.

• A work-hardening/softening law.

The model parameters are assumed to be determined based on direct shear test results performed at different normal stresses and hence, the stress space may be defined by only two independent stress (or strain) variables, τ and σ_n, which are shear and normal stresses respectively. Definitions of model parameters will be presented first. The establishment of the model is then explained afterwards.

Stress Ratio

This is a normalized form of the shear stress to the vertical stress which is used extensively in this developed constitutive model defined as follow:

$$f = \frac{\tau}{\sigma_v} \tag{9}$$

Shear and Axial Strains

Without violating the generality and for consistency between shear and vertical strains and also for convenience, it is assumed that the horizontal displacement on the top of the specimen (at the shear surface) is linearly distributed over the height of the sample in a direct shear test box. Therefore, the shear strain is assumed to be equal to the ratio of horizontal displacement to the height of the box. In the other words, the so called box shear strain, γ_{box}, is used instead of soil shear strain, γ_{soil}, which are shown in schematic representation of a direct shear test in Fig. 4.

It is worth mentioning that the shear strains formed in the sample is often much more than box shear strains. A number of studies have been made to relate box shear strain to soil shear strain by defining a shear band thickness, ts, as a function of soil particles size in which, major part of soil straining occurs. An extensive study of Cerato (2005) shows that this shear band is between 10 to 20 times of the average soil grain size, D_{50} [18].

As a result, a so called shear scaling ratio, rs, can be defined as follow:

$$r_s = \frac{\gamma_{soil}}{\gamma_{box}} \tag{10}$$

This ratio is expected to be more than unity. In the following procedure, the ratio of shear and vertical strains are required for the model and hence, the strain ratio is not a matter of concern until the model is implemented in the ZEL method, where, the scaling ratio can be used to find actual soil shear strain. This ratio can be defined using any suggested equations for shear band thickness in most of practical cases, but care should be taken to the sensitivity of the foundations load-displacement curve to this ratio. It is recommended to adjust this factor by comparing the predicted and observed load-displacement curves of a model footing load test to calibrate the model.

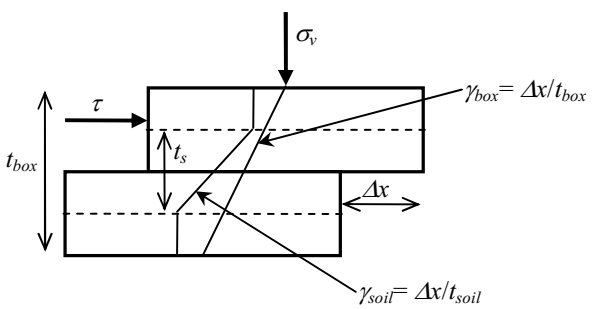

Fig. 4. Representation of box and soil shear strains in a direct shear test

Elastic Behavior

The model is supposed to represent and predict only plastic behavior of the soil regarding the requirements of the ZEL method in which, soil is supposed to yield even at the initiation of the loading. Thus, elastic strains are assumed to be reasonably small and insignificant. Elastic deformations however, can be found from the equation presented by Lade and Duncan (1975) assuming zero Poisson's ratio as follow [24]:

$$E_{ur} = k_{ur}\left(\frac{\sigma_3}{P_a}\right)^n \tag{11}$$

In this equation, E_{ur} is the unloading-reloading modulus, σ_3 is the confining pressure (in a triaxial test), P_a is the atmospheric pressure and n is a coefficient determined from laboratory triaxial tests results. Therefore, other elasticity coefficients for shear stress-shear strain relationship can be simply obtained. For example, shear modulus, G is equal to half of the Young's modulus, i.e., $G=0.5E_{ur}$ which can be used to find shear strains.

Yield Criterion

For simplicity and consistency with the assumptions presumed in the ZEL method, the yield criterion is suggested to be similar in shape to the well-known failure criterion of Coulomb as follows:

$$f_y(\tau, \sigma_v) = \tau - k_1\sigma_v \tag{12}$$

where, k_1 is a variable ranging between 0 (at the initiation of loading) and tan ϕ_{mob} at higher stages of loading. Also, ϕ_{mob} varies during soil shear and it can reach an ultimate value of ϕ_{peak} at peak strength and a constant value of $\phi_{c.s.}$ where experiencing sufficiently large shear deformations. The critical state soil friction angle, $\phi_{c.s.}$, is independent of stress level and supposed to be a material constant for a certain soil type. The factor k_1 which is a function of soil mobilized inter-granular friction angle, can also be considered as a function of soil critical state friction angle, $\phi_{c.s.}$, and soil dilation angle , v. The yield surface is assumed to expand with the stress level during the state of loading. In an unloading case, the material behavior is supposed to be elastic which is not a concern in the ZEL method.

Plastic Potential Function

The plastic potential function incorporated in this model is presumed to be similar in shape to the yield function, as assumed by Lade and Duncan (1975) and many other researchers:

$$g(\tau,\sigma_v)=\tau-k_2\sigma_v$$

where, k_2 is a model parameter that will be defined later from laboratory tests. Therefore, dissimilarity between k_1 and k_2, suggests a non-associative flow rule assumption. It will be shown that this parameter has a physical meaning. As a result, regarding plasticity theory and normality law, the plastic strain increments can be obtained as follows for any component of strains in a general strain configuration [52]:

$$d\varepsilon_{ij}^{p}=d\lambda\frac{\partial g}{\partial\sigma_{ij}} \tag{13}$$

According to the previous notation for stresses in a direct shear test, predefined incremental strains can be found as follow:

$$d\varepsilon^{p}=d\lambda\frac{\partial g}{\partial\sigma_{v}}=d\lambda(-k_2) \tag{14a}$$

$$d\gamma^{p}=d\lambda\frac{\partial g}{\partial\tau}=d\lambda \tag{14b}$$

In these equations, $d\lambda$ is plastic multiplier, ε^p is the incremental plastic normal strain and γ^p is the incremental plastic shear strain. If the value of $d\lambda$ is defined for a given stress ratio, f, incremental plastic strains can be related to incremental stresses and vice versa. Experimental data show that the value of k_2 has a physical meaning. In fact, it is a representation of the rate of dilation when the soil undergoes shear deformations:

$$\frac{d\sigma^{p}}{d\tau^{p}}=\frac{d\theta(\lceil k_2)}{d\theta}=\lceil k_2=\lceil\tan\psi \tag{15}$$

Experimental evidences show that when the value of k_2 is plotted versus the stress ratio, f, they would be located on a straight line. As an example, Lade and Duncan (1975) reported similar observation by performing a triaxial test on sand [24]. To demonstrate this fact, direct shear tests results of Kumar et al. (2007) on Bangalore Sand are presented which have been tested at different relative densities and under different normal stresses in a direct shear box apparatus of 60mm in width and 30.77mm in height (Kumar et al., 2007) [51]. Sand properties are listed in Table 1. As per the Indian Standard for soil classification, this soil is classified as poorly graded sand [51]. Direct shear tests results on this sand at a relatively dense state is presented in Fig. 5. Stress-strain curves at three different vertical stresses, i.e., 50kPa, 200kPa and 800kPa which cover almost the entire range of the tested samples, have been utilized as plotted in Fig. 6.

Table 1. Bangalore Sand properties (Data from Kumar et al., 2007)

Parameter	Value
Silt Content	Insignificant
Specific Gravity, G_s	2.67
Relative Density, D_r	55.6%
Max. Unit Weight	18.1kN/m^3
Min. Unit Weight	14.3kN/m^3
$\phi_{c.s.}$	31.9^o
D_{10}	0.23mm
D_{30}	0.4mm
D_{50}	0.62mm
D_{60}	0.78mm
C_u	3.4
C_c	0.9

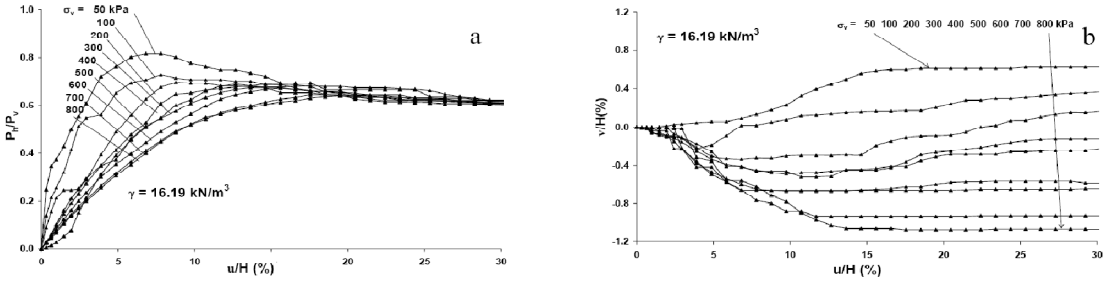

Fig. 5. Direct shear tests results on Bangalore Sand at =16.19kN/m3 (Data from Kumar et al., 2007)

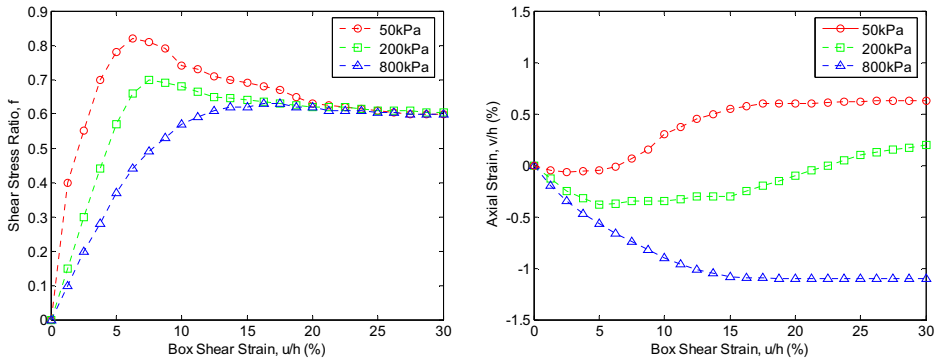

Fig. 6. Selected direct shear test data at γ=16.19kN/m^3

Values of k_2 have been computed and observed to obey a linear relationship when it is plotted versus the stress ratio, f. This is shown in Fig. 7. Therefore, having known the relationship between the parameter k_2 and the stress ratio, f, the value of k_2, defining the plastic potential function, can be evaluated at any given stress ratio. It can be expressed by the following equation:

$$k_2 = Af + H \tag{16}$$

In this equation, A and H are model constants that can be determined experimentally, for instance, A being the slope of the k_2-f line, and H the vertical intercept.

Work-Hardening/Softening Law

At this point, it is necessary to find the magnitudes of strain increments caused by the stress increments. The work used to produce plastic yield is termed the work-hardening law. They also stated that the adaptation of an isotropic hardening law implies that the yield surface can expand uniformly and the hardening degree doesn't depend on the stress path. Therefore there exist a unique relationship between the total plastic work and the degree of hardening which can be expressed by a stress ratio [24]. Total plastic work can also be expressed as follow according to plasticity theories [52]:

$$W_p = \int \left[\sigma_{ij}\right]^T \left[d\varepsilon_{ij}^p\right] \tag{17}$$

In this equation, $\left[\sigma_{ij}\right]^T \left[d\varepsilon_{ij}^p\right]$ is the plastic work done per unit volume of the soil element over the strain increment, $d\varepsilon_{ij}^p$. By differentiating both sides of this equation and substituting the corresponding values for plastic strain increments the following expression can be resulted:

$$dW_p = d\theta \left[\sigma_{ij}\right]^T \Rightarrow \frac{\partial g}{\partial \sigma_{ij}} + \tag{18}$$

For the case of direct shear test where one may use two independent stress variables this equation may be rewritten as follow:

$$dW_p = d\lambda\left(\tau\frac{\partial g}{\partial \tau} + \sigma_v \frac{\partial g}{\partial \sigma_v}\right) = d\lambda(1-k_2)$$

$$\Rightarrow d\lambda = \frac{dW_p}{1-k_2} \tag{19}$$

This is a fairly simple equation relating the value of $d\lambda$ to the plastic work increment, dW_p, at each increment of loading. Now, if the plastic work is related to the stress ratio, f, a complete constitutive model can be established. To do this, first the total normalized plastic work (W_p/P_a) done in the tests are plotted versus the values of the stress ratio, f, during the tests. P_a is the atmospheric pressure used for non-dimensional representation. This is shown in Fig. 8.

Looking at the plotted data, one may arrive at the conclusion that the W_p-f relationship can be approximated by a 3rd-order hyperbolic function that can provide both forms of dilative and contractive behaviors. The idea behind this assumption is that such function can capture a peak value of f and provide a constant value for this parameter at reasonably large shear strains. Therefore, the following form of this function is suggested:

$$f = \frac{aW_p^3 + bW_p}{W_p^3 + c} \tag{20}$$

In this equation, a, b and c are model parameters that should be determined from laboratory test results. There is a brief explanation on the role of each of these parameters in the following parts:

Parameter a:

This parameter is rather more important than the others and controls the final part of the f-W_p curve, i.e. the value of f at infinity. Since at infinity (very high shear strains), f approaches the value corresponding to the soil critical state condition (or at failure), this parameter should be set equal to f at the critical state:

$$\lim_{W_p \to \infty} f = a = \tan\phi_{c.s.} \tag{21}$$

Therefore, parameter a can easily be determined from experimental data.

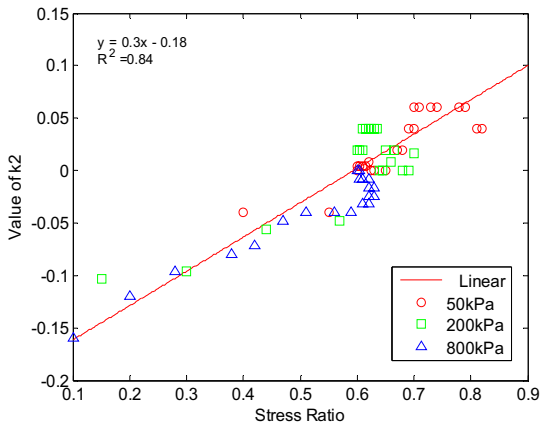

Fig. 7. Relationship between the value of k_2 and stress ratio

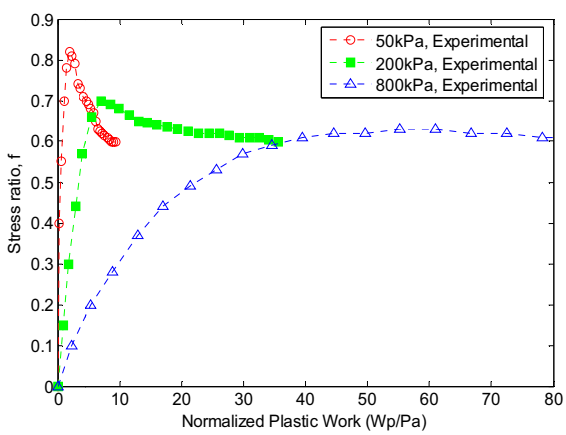

Fig. 8. Variations of stress ratio with normalized plastic work, W_p/P_a

Parameters b:

This parameter controls the magnitude of the maximum value of the stress ratio, *f*. It can be seen in Fig. 9a for constant values of parameters *a* and *c*. This parameter should be considered in conjunction with the last parameter, c.

Parameter c:

This parameter controls the location of the peak value in conjunction with the parameter b. The role of the parameter *c* is shown in Fig. 9b which affects the extension, sharpness and in general, the shape of the hyperbola. To provide a brief representation of this parameter, the derivation of the suggested hyperbolic equation is as follow:

$$\frac{df}{dW_p} \psi \frac{(3aW_p^2 \theta b)(W_p^3 \theta c) \sigma 3W_p^2(aW_p^3 \theta bW_p)}{(W_p^3 \theta c)^2} \tag{22}$$

$$\tau \quad \frac{df}{dW_p} \psi \frac{\sigma bW_p^2 \theta 2acW_p \theta bc}{(W_p^3 \theta c)^2}$$

At the beginning of the curve, the slope of the curve is as follows:

$$\Rightarrow \left.\frac{df}{dW_p}\right|_{W_p=0} = \frac{bc}{c^2} = \frac{b}{c} \tag{23}$$

There is also similar relationship for the peak value in which, the first derivative of the hyperbola is zero. Hence, there would be two equations for two unknowns, i.e. *b* and *c* for each test and hence, they can be determined.

Therefore, these parameters can be determined as functions of stress level (i.e. vertical stress) from laboratory shear tests. In summary, to determine these parameters, one should find the peak value of the plastic work at each test and compute the initial slope of the f-W_p curves.

As a conclusion, the model parameters can be summarized as follows:

- Elastic coefficients (Similar to other linear elastic models which are not required here).
- Yield criterion parameters: $k_1 = tan\phi_{mob}$.
- Failure criterion: $k_{1\text{-}failure} = tan\phi_{c.s}$. (from laboratory shear tests)
- Plastic potential function parameters: k_2 (function of f, expressed in terms of A and H)
- Work hardening/strain softening law: a, b and c coefficients
  - o $a = tan\phi_{c.s.} = k_{1\text{-}failure}$
  - o b and c from tests results (initial slopes and peak value of the W_p-f curves, functions of vertical stress)

Therefore, there are total of 6 parameters which can be summarized into 5 independent parameters: A, H, $tan\phi_{c.s.}$ (equal to a), b and c.

Computation Steps

After evaluation of the model parameters, it is necessary to follow a computational procedure to find the stress-strain curve of a certain test. To do this the following steps should be followed:

- Given values are: σ_v, a (equal to $tan\phi_{c.s.}$), b, c (as functions of σ_v/P_a), A and H.
- Application of a shear stress increment, $d\tau$
- Finding the total value of the shear stress, $\tau = \tau_0 + \Delta\tau$, and τ_0 is the previous value of τ.
- Computing the stress ratio, $f = \tau/\sigma$
- Computing the value of k_2.
- Finding appropriate value of W_p corresponding to the current stress ratio, f.
- Computation of the plastic work increment: $\Delta W_p = W_p - W_{p0}$, in which, W_{p0} is the plastic work of the previous step.
- Computing the plastic potential function at the current stress ratio.
- Finding corresponding value of $\Delta\lambda$.
- Computation of the shear strain and axial strain based on plasticity equations.

This procedure can be simply programmed for practical purposes. A computer code in MATLAB has been provided for the computation procedure and used as a supplementary function in a developed code for solution of the ZEL equations.

Verification

These parameters have been evaluated for the tests performed by Kumar et al. (2007) and shown in Table 1 and Fig. 10. It is realized that the model parameters are in a very reasonable consistency when a power law equation is fitted to them on a log-log scale plot. Test results at 50, 200 and 800kPa

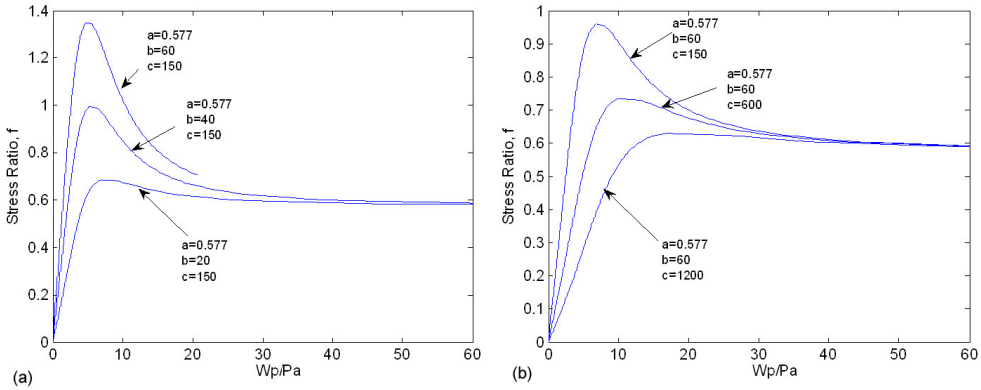

Fig. 9. Role of the parameters in the suggested hyperbolic function in development of the constitutive model: a) variations of *b* and b) variations of *c*

Table 2. Evaluation of the model parameters in each test

Test No.	σ_v (kPa)	$\phi_{c.s.}$ (Deg.)	A	H	a	b	c
1	50	31.9	0.3	-0.18	0.62	4	8
2	200	31.9	0.3	-0.18	0.62	30	250
3	800	31.9	0.3	-0.18	0.62	190	9000

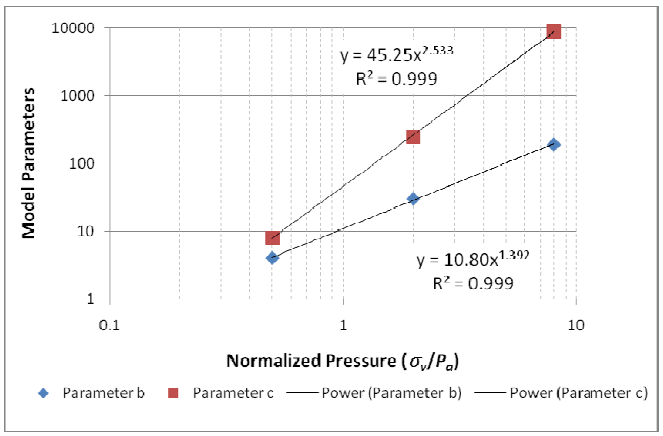

Fig. 10. Evaluation of the model parameters

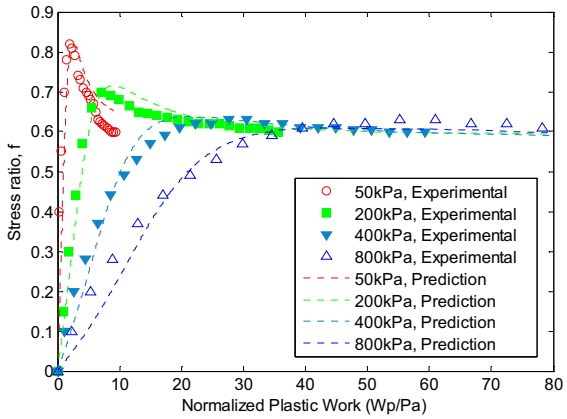

Fig. 11. Calibration of the model parameters

vertical stresses were used for model calibration and the results of 400kPa vertical stress were kept for verification.

Also, using the plot of k_2 against the stress ratio, f, the following relationship can be obtained:

$$k_2=0.3f-0.18 \quad (24)$$

Using these parameters and equation for k_2, plastic work curve for each test is computed and plotted in Fig. 11 for vertical stresses of 50, 200, 800kPa (used for calibration) and 400kPa (used for verification). It can be well observed that the model can reasonably capture the plastic work variations.

Now, the model is utilized to provide a complete stress-strain curve. Using these values, an incremental shear stress was applied for each normal stress at each test and the corresponding values of plastic strain increments were computed. A comparative plot of the model prediction and experimental results are shown in Fig. 12. In this figure, stress-strain curves at the vertical stresses equal to 50 and 200kPa which were previously used for model calibration and at the vertical stress of 400kPa, which were taken to verify the model, are depicted. The ability of the model in prediction of the test results seems to be reasonable.

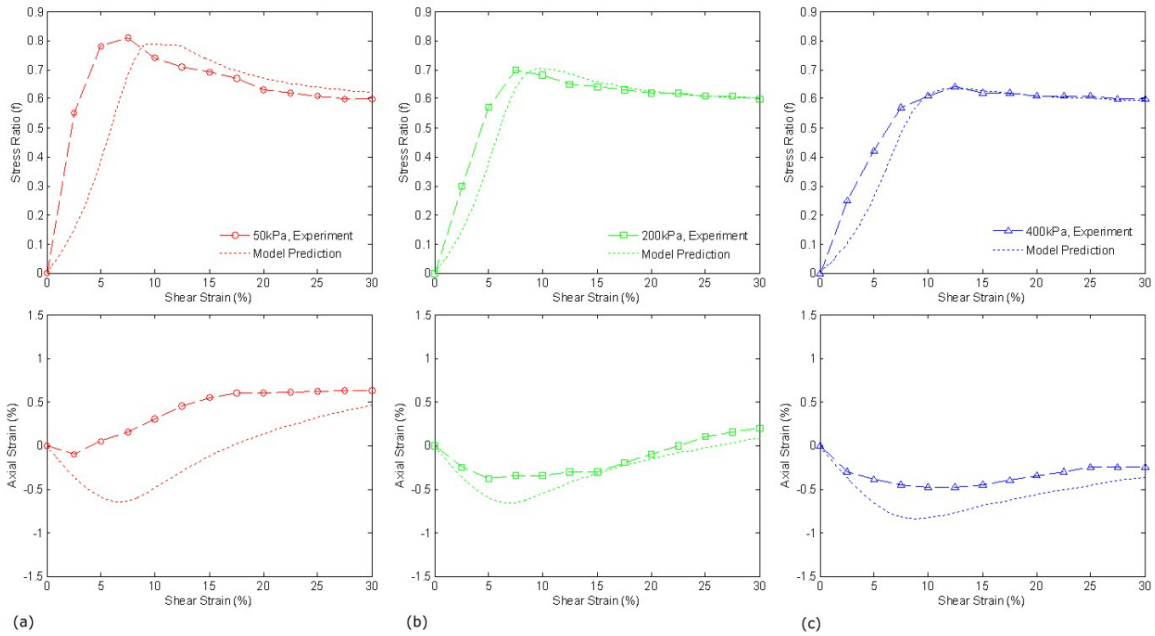

Fig. 12. Direct shear tests, experimental and model predicted results:
a) σ_V=50ka (for calibration), b) σ_V=200ka (for calibration) and c) σ_V=400ka (for verification)

4. Foundations Behavior Investigation

As stated earlier, foundations behavior is stress level dependent which can be related to the foundation size. The developed constitutive model can provide a suitable tool to describe both dilative and contractive soil behaviors and as a result, can be utilized to predict foundations behavior. The ZEL method which can consider the stress level dependency of soil shear strength parameters is employed to investigate foundations behavior. The developed constitutive soil model has been implemented in this method in which, the relationship between $\sin\phi_{mob}$. and γ_{xy} is available at every stress level. Numerical investigation of foundations behavior has been performed by using the direct shear tests results presented earlier.

Contribution of the Constitutive Model and Computation Procedure

Computation procedure is as follow:

• First it is necessary to construct the ZEL field. It can be done by simultaneous solution of the finite difference forms of the ZEL equations presented in Appendix A. A computer code has been developed in this research to solve these equations. It should be noted that the boundary condition of Bolton and Lau (1993) has been adopted for computations in which, formation of a relatively rigid wedge (or cone, in axi-symmetric problems) beneath the foundation is assumed [6]. According to the test results and predictions of the model, average soil angle of dilation was assumed to be a function of stress level ranging approximately between 5 to 15 degrees. This is shown in Fig. 13.

• At an arbitrary displacement increment in the analysis, e.g. vertical displacement of the foundation, the velocity and strain fields are obtained by the aid of the ZEL method. Outline of such an analysis is described well in the literature [36-40]. Therefore, at an arbitrary foundation displacement, the shear strains are readily determined within the soil mass. Also, the previous values of soil mobilized friction angles and stresses are known. These values can be used as initial values to find updated stresses and corresponding mobilized friction angles at each node of the ZEL net.

• The input parameters for the constitutive soil model which is implemented in the ZEL method at the i^{th} step of computation are as follow:

o S_{i-1}, mean stress value of the previous step.

o ϕ_{i-1}, mobilized friction angle of the previous step.

o γ_{max}, maximum shear strain generated in the current step.

• Now, having known the stress state of the previous step, it is required to find the corresponding stress state (and mobilized friction angle) for the current step.

• First, it is necessary to find the direction of the shear plane. As stated earlier, it has been found that this plane makes an angle equal to $\mu=\pi/4-\phi_{mob}./2$ with the minor principal stress plane. Therefore, according to Fig. 14, the shear stress, τ_{sp}, and normal stress (required to compute model parameters), σ_{sp}, at the shear plane can be found easily as follow:

$$\tau_{sp}=(S\sin\phi_{mob})\sin 2\mu$$
$$\sigma_{sp}=S-(S\sin\phi_{mob})\sin 2\mu$$

• Second, the corresponding value of the shear strain at shear plane, γ_{max}, should be determined knowing the angle, by the following relationship according to Fig. 14b:

$$\gamma_{max}=\gamma_{max}\sin 2\mu$$

Having known the vertical stress, constitutive model parameters, i.e. b, c and k_2, which are functions of vertical stress and stress ratio, can also be determined. Other parameters, i.e. a (equal to $\tan\phi_{c.s.}$), A and H, are stress level independent and remain unchanged. Initial value of the mobilized soil friction angle may be used for primary results and after sufficient iterations, the corresponding value of the mobilized friction angle will be found which is the output of the model into the ZEL method.

• The procedure is repeated for next and next steps of loading and displacement to find a complete load-displacement curve for the foundation.

• Regarding the shear box size and soil average grain size, a shear strain ratio, $r_s=3$ was adopted for the analyses.

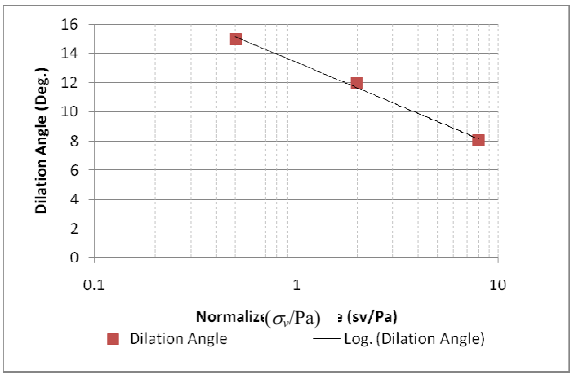

Fig. 13. Variations of soil angle of dilation

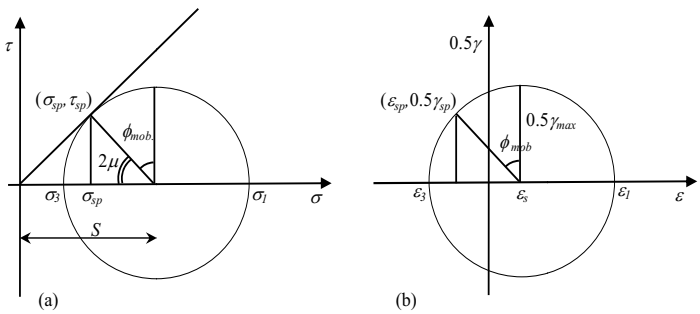

Fig. 14. Mohr's circle of a) stresses and b) strains; to find σ_{sp} and γ_{sp}

Results

Behavior of foundations of different sizes on the presented relatively dense sand have been investigated. Fig. 15 shows the ZEL net, load-displacement curve and the velocity field for a circular foundation 1.0m in diameter having a rough base. There is an obvious peak corresponding to a general shear failure mode of rupture. Fig. 16 shows similar results for a relatively large foundation of 50m diameter. It can be seen that there is rather no apparent peak value in the load-displacement curve and hence, the failure mechanism should be more localized. Load-displacement curves of different size foundations are shown in Fig. 17 for comparison. The figure indicates a peak in load-deflection behavior of small footings which diminishes with increase in footing size. This is consistent with the observations of Clark (1996) in his centrifuge tests [16].

A plot of the foundations ultimate bearing capacity obtained from the analyzed cases in this study is provided and shown in Fig. 18 on a log-log scale. The results indicate that the bearing capacity decreases almost linearly with logarithmic increase in foundation size. Such fact is in agreement with experimental observations found in the literature.

In many practical problems, the bearing capacity of shallow foundations is often computed from the bearing capacity equation. In more important projects, it is conventional to perform a small scale or plate load test and extrapolate the results to larger foundations due to difficulties in performing full scale load tests. There are several delusions in using theoretical methods or extrapolation of small scale tests results for larger foundations as stated by the researchers [15,53,54]. It is suggested by Fellenius and Altaee (1994) that when the small scale footing load tests results are extrapolated, a stress scale should also be considered rather than a geometric scaling alone [15].

The effect of stress level or foundation size has been considered in the zero extension line method for calculation of ultimate bearing capacity [55,56], but the load-deflection curve of a footing provides a more meaningful picture of its behavior as well as its capacity in bearing the loads at the ultimate states. Since the main goal of the current work was to

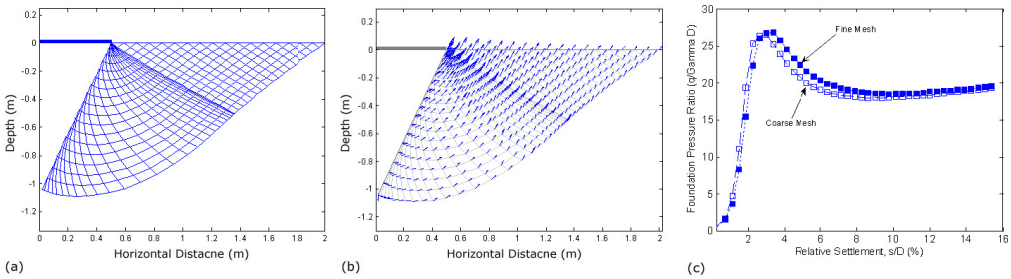

Fig. 15. Results for a circular foundation with rough base, (D=1.0m):
a) ZEL net, b) Velocity field and c) Load-displacement curve

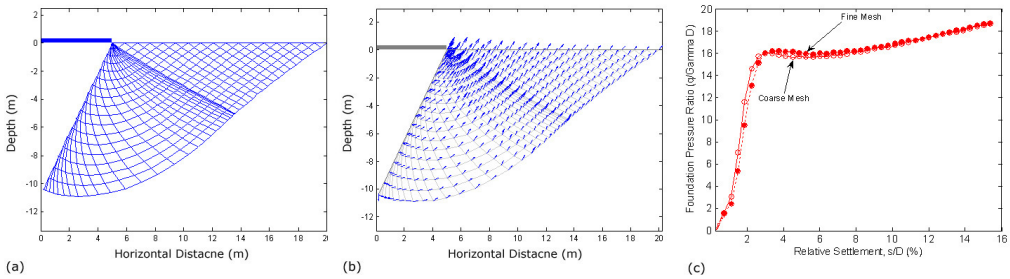

Fig. 16. Results for a circular foundation with rough base, (D=50m):
a) ZEL net, b) Velocity field and c) Load-displacement curve

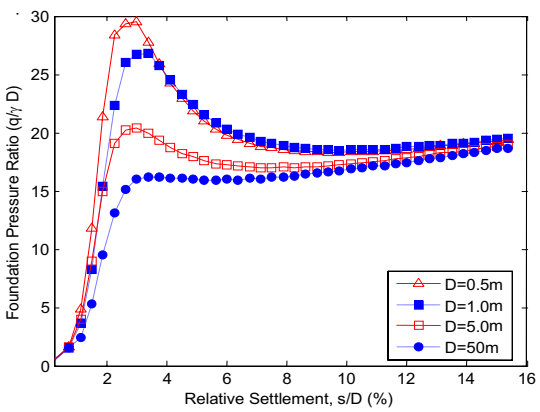

Fig. 17. Comparison between different size foundations behaviors

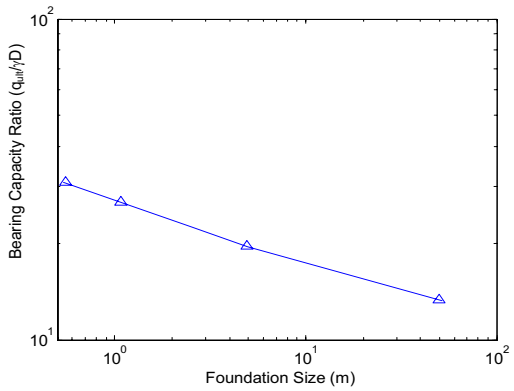

Fig. 18. Variations of the ultimate bearing capacity ratio with foundation size

present a soil constitutive model for implementation into the zero extension line method, verification has been made for the model itself. It was also shown that the predicted load-deflection behavior of small and large footings is different from each other. This behavior is consistent with the observations made in centrifuge tests [16]. Quantitative verification of the predictions of the model against full scale tests that has been performed up to failure states was not possible in the course of this study. Result of such investigations has been presented independently [57,58].

5. Conclusions

The ultimate bearing capacity of shallow foundations has been well recognized and the triple-N equation of Karl Terzaghi (1943) is widely used by assuming a constant soil friction angle, to determine the ultimate bearing capacity. However, observations indicate the stress level dependency of soil friction angle, and thus, a unique relationship between the ultimate bearing capacity of shallow foundations and soil friction angle does not exist. As a matter of fact, variations of soil friction angle arising from stress level dependent soil behavior, should be considered in prediction of foundations behavior. In this research, a rather simple work hardening/softening constitutive soil model is developed which is capable of capturing both dilational and contractive soil behaviors. Model parameters can be determined from standard laboratory direct shear tests on frictional soils performed at different vertical stresses. The model was formulated and verified with experimental results of Kumar et al. (2007) data, showing reasonable advantages. This model was then implemented into the ZEL method to investigate the load-displacement behavior of shallow foundations. Utilization of this model enables the ZEL method to capture different modes of foundations behavior due to foundation size effect. A numerical study revealed that increase in foundation size leads to a transition in foundations behavior and modes of failure, from general shear failure to localized shear failure mechanism. Values of the ultimate bearing capacity of foundations plotted versus foundations size on a log-log scale coincide with the previous experimental observations indicating a linear relationship, i.e., the decrease in the bearing capacity with increase in the foundation size.

In conclusion, developed constitutive soil model can be reasonably employed in the ZEL method to describe and predict actual foundation behaviors. This model is relatively simple and requires only the direct shear test results for calibration, which is a simple and commonly used test for frictional soils.

Acknowledgement: The authors would like to extend their appreciations to Prof. N. Hataf and Prof. G. Habibagahi, faculty members of Shiraz University, for their scientific supports of the second author.

References

[1] K. Terzaghi, Theoretical Soil Mechanics, John-Wiley and Sons Inc., NY, 1943.

[2] J. E. Bowles, Foundation Analysis and Design, 5th Ed., New York: McGraw-Hill Co., 1996.

[3] G. G. Meyerhof, "Some Recent Research on the Bearing Capacity of Foundations", Can. Geotech. J. 1: 16-26, 1963.

[4] J. B. Hansen, "A Revised and Extended Formula for Bearing Capacity", Danish Geotechnical Institute, Copenhagen, Bulletin, 28: 5-11, 1970.

[5] A. S. Vesi?, "Analysis of Ultimate Loads of Shallow Foundations", Journal of the Soil Mechanics and Foundations Division, ASCE 99: 45-73, 1973.

[6] M. D. Bolton and C. K. Lau, "Vertical Bearing Capacity Factors for Circular and Strip Footings on Mohr-Coulomb Soil", Can. Geotech. J. 30: 1024-1033, 1993.

[7] R. L. Michalowski, "An Estimate of the Influence of Soil Weight on Bearing Capacity Using Limit Analysis", Soils and Foundations, Japanese Geotechnical Society, Vol.37, No.4, pp.57-64, Dec. 1997.

[8] J. Kumar, "N for Rough Strip Footing Using the Method of Characteristics", Can. Geotech. J., 40 (3): 669-674, 2003.

[9] J. Kumar and P. Ghosh, "Bearing Capacity Factor N for Ring Footings Using the Method of Characteristics", Can. Geotech. J., 42: 1474-1484, 2005.

[10] M. Hjiaj, A. V. Lyamin and S. W. Sloan, "Bearing Capacity of a Cohesive-Frictional Soil under Non-Eccentric Inclined Loading," Computers and Geotechnics, Elsevier, 31 (2004): 491-516.

[11] M. Hjiaj, A. V. Lyamin and S. W. Sloan, "Numerical Limit Analysis Solutions for the Bearing Capacity Factor N ," Int'l Journal of Solids and Structures, Elsevier, 42 (2005): 1681-1704.

[12] E. E. De Beer, "Bearing Capacity and Settlement of Shallow Foundations on Sand", In Proc. of the Bearing Capacity and Settlement of Foundations Symposium, Duke University, Durham, N.C., pp.15-34, 1965.

[13] N. K. Ovesen, "Centrifugal Testing Applied to Bearing Capacity Problems of Footings on Sand", Géotechnique, 25 (2): 394-401, 1975.

[14] M. D. Bolton and C .K. Lau, "Scale Effect in the Bearing Capacity of Granular Soils," In Proc. Of the 12th Int'l Conf. on Soil Mech. Found. Eng., Rio De Janeiro, Brazil, Vol.2, pp.895-898, 1989.

[15] B. H. Fellenius and A. Altaee, "Stress and Settlement of Footings in Sand," In Proc. of the American Society of Civil Engineering, ASCE, Conference on Vertical and Horizontal Deformations for Foundations and Embankments, Geotechnical Special Publication, GSP, No. 40, College Station, TX, June 16-18, 1994, Vol. 2, pp. 1760-1773.

[16] J. I. Clark, "The Settlement and Bearing Capacity of Very Large Foundations on Strong Soils: 1996 R.M. Hardy Keynote Address", Can. Geotech. J., 35: 131-145, 1998.

[17] F. Zhu, J. I. Clark, and R. Phillips, "Scale Effect of Strip and Circular Footings Resting on Dense Sand", Journal of Geotechnical and Geoenvironmental Engineering, ASCE, Vol.127, No.7, July 2001, pp.613-621.

[18] A. B. Cerato, and A. J. Lutenegger, "Bearing Capacity of Square and Circular Footings on a Finite Layer of Granular Soil Underlain by a Rigid Base", Journal of Geotechnical and Geoenvironmental Engineering, ASCE, Vol.132, No.11, November 2006, pp.1496-1501.

[19] A. B. Cerato, and A. J. Lutenegger, "Scale Effects of Shallow Foundation Bearing Capacity on Granular Material", Journal of Geotechnical and Geoenvironmental Engineering, ASCE, Vol.133, No.10, October 2007, pp.1192-1202.

[20] J. Kumar and V. N. Khatri, "Effect of Footing Width on Bearing Capacity Factor, N " Journal of Geotechnical and Geoenvironmental Engineering, ASCE, Vol.134, No.9., Sept. 2008, pp.1299-1310.

[21] H. B. Poorooshasb, I. Holubec, and A. N. Sherbourne, "Yielding and Flow of Sand in Triaxial Compression (Part I)", Can Geotech. J., 3, 4, 1966, pp. 179-190.

[22] H. B. Poorooshasb, I. Holubec, and A. N. Sherbourne, "Yielding and Flow of Sand in Triaxial Compression (Parts II and III)", Can Geotech. J. 4, 4, 1967, pp. 376-397.

[23] R. Nova, and D. M. Wood, "A Constitutive Model for Sand in Triaxial Compression", Int'l. J. Num. Anal. Meth. Geomech,. 3, 3, 1979, pp. 255-278.

[24] P. V. Lade and J. M. Duncan, "Elastoplastic Stress-Strain Theory for Cohesionless Soil", Journal of the Geotechnical Engineering Division, ASCE, Vol. 101 (GT10), 1975, pp.1037-1053.
[25] K.-H. Yang, C. D. L. Nogueira, and J. G. Zornberg, "Isotropic Work Softening Model for Frictional Geomaterials: Development Based on Lade and Kim Constitutive Model", XXIX CILAMCE Iberian Latin American Congress on Computational Methods in Engineering, November 4th to 7th, 2008.
[26] Hamidi, A., Alizadeh, M. and Soleimani, S. M., "Effect of Particle Crushing on Shear Strength and Dilation Characteristics of sand-Gravel Mixtures", International Journal of Civil Engineering, Vol. 7, No. 1, March 2009.
[27] Sadrnejad, S. A. and Ghoreishian Amiri, S. A., "A Simple Unconventional Plasticity Model Within the Multilaminate Framework", International Journal of Civil Engineering, Vol. 8, No. 2, June 2010.
[28] Baziar, M. H., Ghorbani, A. and Katzenbach, R., "Small-Scale Model Test and Three-Dimensional Analysis of Pile-Raft Foundation on Medium-Dense Sand", Vol. 7, No. 3, September 2009.
[29] R. Guo and G. Li, "Elasto-Plastic Constitutive Model for Geotechnical Materials with Strain-Softening Behaviour", Computers and Geotechnics, 34 (2008): 14-23.
[30] N. Yamamoto, M. F. Randolph and I. Einav, "Numerical Study of the Effect of Foundation Size for a Wide Range of Sands", Journal of Geotechnical and Geoenvironmental Engineering, ASCE, Vol.135, No.1, January 2009, pp.37-45.
[31] N. Yamamoto, Numerical Analysis of Shallow Circular Foundations on Sands, Ph.D. Dissertation Submitted to the School of Civil and Resource Engineering, The University of Western Australia, May 2006.
[32] J. M. Pestana, and A. J. Whittle, "Compression Model for Cohesionless Soils", Géotechnique, 45(4): 611-631, 1995.
[33] J. M. Pestana, A. J. Whittle, and L. A. Salvati, "Evaluation of a Constitutive Model for Clays and Sands, Part 1: Sand Behaviour", International Journal for Numerical and Analytical Methods in Geomechanics, 26(11): 1097-1121, 2002.
[34] K. H. Roscoe, "The Influence of Strains in Soil Mechanics", Tenth Rankine Lecture, Géotechnique, 20 (2): 129-170, 1970.
[35] R. G. James and P. L. Bransby, "A Velocity Field for Some Passive Earth Pressure Problems," Géotechnique, 21 (1): 61-83, 1971.
[36] K. Habibagahi, and A. Ghahramani, "Zero Extension Line Theory of Earth Pressure," Journal of the Geotechnical Engineering Division, ASCE, Vol.105, No.GT7, July 1979, pp. 881-896.
[37] A. Ghahramani, and S. P. Clemence, "Zero Extension Line Theory of Dynamic Passive Pressure," Journal of the Geotechnical Engineering Division, ASCE, Vol.106, No.6, June 1980, pp. 631-644.
[38] M. Jahanandish, L. Behpoor, and A. Ghahramani, "Load-Displacement Characteristics of Retaining Walls." In Proc. Of the 12th Int'l Conf. on Soil Mech. Found. Eng., Rio De Janeiro, Brazil, Vol. 1, pp. 243-246, 1989.
[39] S. A. Anvar and A. Ghahramani, "Equilibrium Equations on Zero Extension Lines and Their Application to Soil Engineering," Iranian Journal of Science and Technology (IJST), Shiraz University Press., Transaction B, Vol.21, No.1, pp.11-34, 1997.
[40] M. Jahanandish, "Development of a Zero Extension Line Method for Axially Symmetric Problems in Soil Mechanics," Scientia Iranica Journal, Sharif University of Technology Press., Vol.10, No.2, pp.1-8, 2003.
[41] M. Jahanandish, S. M. Mansoorzadeh and K. Emad, "Zero Extension Line Method for Three-dimensional Stability Analysis in Soil Engineering," Iranian Journal of Science and Technology (IJST), Shiraz University Press., Transaction B, Vol.34, No.B1, pp.63-80, 2010.
[42] D. M. Wood, Soil Behavior and Critical State Soil Mechanics, Cambridge University Press, 1990, 480p.
[43] J. Atkinson, The Mechanics of Soils and Foundations, 2nd Ed., Routledge, Taylor and Francis Group, 2008, 475p.
[44] G. G. Meyerhof, The Bearing Capacity of Sand, Ph.D. Thesis, University of London, London, England, 1950.
[45] E. E. De Beer, "Bearing Capacity and Settlement of Shallow Foundations on Sand", In Proc. of the Bearing Capacity and Settlement of Foundations Symposium, Duke University, Durham, N.C., pp.15-34, 1965.
[46] K. L. Lee and H. B. Seed, "Drained Strength Characteristics of Sands", Journal of the Soil Mechanics and Foundations Division: Proceedings of the American Society of Civil Engineers, ASCE. Vol. 93, No. SM6, pp. 117-141, 1967.
[47] M. D. Bolton, "The Strength and Dilatancy of Sands", Géotechnique, 36: 65-78, 1986.
[48] J. K. M. Gan, D. G. Fredlund and H. Rahardjo, "Determination of the Shear Strength parameters of an Unsaturated Soil Using the Direct Shear Test", Can. Geotech. J. 35: 500-510, 1988.
[49] K. Maeda and K. Miura, "Confining Stress Dependency of Mechanical Properties of Sands", Soils Foundations, Japanese Geotechnical Society, Vol. 39, No. 1, pp. 53-67, 1999.
[50] M. Budhu, Soil Mechanics and Foundations, 2nd Ed., John Wiley and Sons, 2007.
[51] J. Kumar, K. V. S. B. Raju and A. Kumar, "Relationships between Rate of Dilation, Peak and Critical State Friction Angles", Indian Geotechnical Journal, 37 (1) 2007, pp.53-63.
[52] H.-S. Yu, Plasticity and Geotechnics, Springer, 2006.
[53] B. H. Fellenius, "Bearing Capacity of Footings and Piles- A Delusion?" DFI Annual Meeting, October 14-16, 1999, Dearborn, Michigan, U.S.A.
[54] A. Eslami, B. H. Fellenius, and M. Veiskarami, "Problems on Determination of Shallow Foundations Bearing Pressure by Analytical Approach," In Proc. of the 1st National Congress of Civil Engineering (NCCE, 2004), Sharif University of Technology, Tehran, Iran, 2004.
[55] M. Jahanandish, M. Veiskarami and A. Ghahramani, "Effect of Stress Level on the Bearing Capacity Factor N , by the ZEL Method," KSCE Journal of Civil Engineering, Vol. 14, No. 5, pp. 709-723, 2010.
[56] M. Veiskarami, M. Jahanandish and A. Ghahramani, "Application of the ZEL Method in Prediction of Foundations Bearing Capacity Considering Stress level Effect," Soil Mechanics and Foundation Engineering, Vol. 47, No. 3, pp. 75-85, 2010.
[57] M. Veiskarami, M. Jahanandish and A. Ghahramani, "Prediction of Foundations Behavior by a Stress Level Based Hyperbolic Soil Model and the ZEL Method", Journal of Computational Methods in Civil Engineering, Vol. 1 No. 1 pp. 37-54, 2010.
[58] M. Veiskarami, M. Jahanandish and A. Ghahramani, "Prediction of the Bearing Capacity and Load-Displacement Behavior of Shallow Foundations by Stress-Level-Based ZEL Method", Scientia Iranica Journal, Vol. 18, No. 1, pp. 16-27, 2011.

Appendix A: Finite Difference Forms of the Equations and Flowchart of the Procedure

There are four equations and four unknowns at each point, e.g., for an arbitrary point like *C*. Calculations should be performed to find the unknowns at this point from existing data of the previous two points, namely *A* and *B*. For terms without a subscript index, the averaged values between two successive points should be used. For example, angle ψ is initially set equal to ψ_A and after the first round of iterations, it is set equal to averaged value of ψ_A and ψ_C along the positive direction. The finite difference forms of the equations are as follow:

$$\begin{cases} \text{For +tive ZEL:} \dfrac{(z_C - z_A)}{(x_C - x_A)} = \tan(\psi + \xi) \\ \text{For -tive ZEL:} \dfrac{(z_C - z_B)}{(x_C - x_B)} = \tan(\psi - \xi) \end{cases} \quad \text{(A1)}$$

Jahanandish (2003) Equations:

$$\begin{cases} \text{Along the plus (+) ZEL:} \\ (S_C - S_A) + \dfrac{(T_C - T_B)}{\Delta_{BC}}\Delta_{AC} + \dfrac{2T}{\cos\nu}((\psi_C - \psi_A) - \sin\nu\dfrac{(\psi_C - \psi_B)}{\Delta_{BC}}\Delta_{AC}) = [f_r\cos(\psi+\xi) + f_z\sin(\psi+\xi)]\Delta_{AC} \\ \text{Along the minus (-) ZEL:} \\ (S_C - S_B) + \dfrac{(T_C - T_A)}{\Delta_{AC}}\Delta_{BC} - \dfrac{2T}{\cos\nu}((\psi_C - \psi_B) - \sin\nu\dfrac{(\psi_C - \psi_A)}{\Delta_{AC}}\Delta_{BC}) = [f_r\cos(\psi-\xi) + f_z\sin(\psi-\xi)]\Delta_{BC} \end{cases} \quad \text{(A2)}$$

$$\begin{cases} \Delta_{AC} = \sqrt{(x_A - x_C)^2 + (z_A - z_C)^2} = d\varepsilon^+ \\ \Delta_{BC} = \sqrt{(x_B - x_C)^2 + (z_B - z_C)^2} = d\varepsilon^- \end{cases} \quad \text{(A3)}$$

Displacement Equations:

$$dudr + dvdz = 0$$
$$\Rightarrow \begin{cases} (u_{B2} - u_{A2})(r_{B2} - r_{A2}) + (v_{B2} - v_{A2})(z_{B2} - z_{A2}) = 0 \\ (u_{B2} - u_{A3})(r_{B2} - r_{A3}) + (v_{B2} - v_{A3})(z_{B2} - z_{A3}) = 0 \end{cases} \quad \text{(A4)}$$

Shear strain computation can be done by the following equation [58]:

$$\gamma_{rz} = \frac{\left(\cos(\psi+\xi)\dfrac{\partial u}{\partial\varepsilon^-} - \cos(\psi-\xi)\dfrac{\partial u}{\partial\varepsilon^+} - \sin(\psi+\xi)\dfrac{\partial v}{\partial\varepsilon^-} + \sin(\psi-\xi)\dfrac{\partial v}{\partial\varepsilon^+}\right)}{\cos\nu} \quad \text{(A5)}$$

Therefore, the finite difference form of this equation will be as follow:

$$\gamma_{rz} = \frac{\left(\cos(\psi+\xi)\dfrac{u_C - u_B}{\Delta_{BC}} - \cos(\psi-\xi)\dfrac{u_C - u_A}{\Delta_{AC}} - \sin(\psi+\xi)\dfrac{v_C - v_B}{\Delta_{BC}} + \sin(\psi-\xi)\dfrac{v_C - v_A}{\Delta_{AC}}\right)}{\cos\nu} \quad \text{(A6)}$$

Finite difference forms of the ZEL equations are programmed as supplementary functions in the developed computer code. The following supplementary functions have been coded:

- Function ZELCALC: In this function, the ZEL directions are first computed from Eq. A1 and then, the stresses are computed from Eq. A2 and Eq. A3. An iterative procedure is carried out for convergence since the values of ψ are stress dependent and therefore, coordinates of the third point, C, depend on the computed stresses.
- Function DISCALC: In this function, the displacement field is computed. When the displacement boundary is known, a similar triple point strategy is performed to solve two unknown displacement components of point *C*, namely, u_c and v_c by Eq. A4. In the same function, maximum shear strains at each point are also computed by using Eq. A6.
- Function PHIFUN: In this function, a soil model can be inserted to compute the appropriate values of soil mobilized friction angle as a function of both stress level and maximum shear strain.

A general iterative procedure is also carried out over the entire loop (at each displacement step) until no significant change is observed in the values of stresses and other unknowns. The flowchart of the calculation procedure is outlined below:

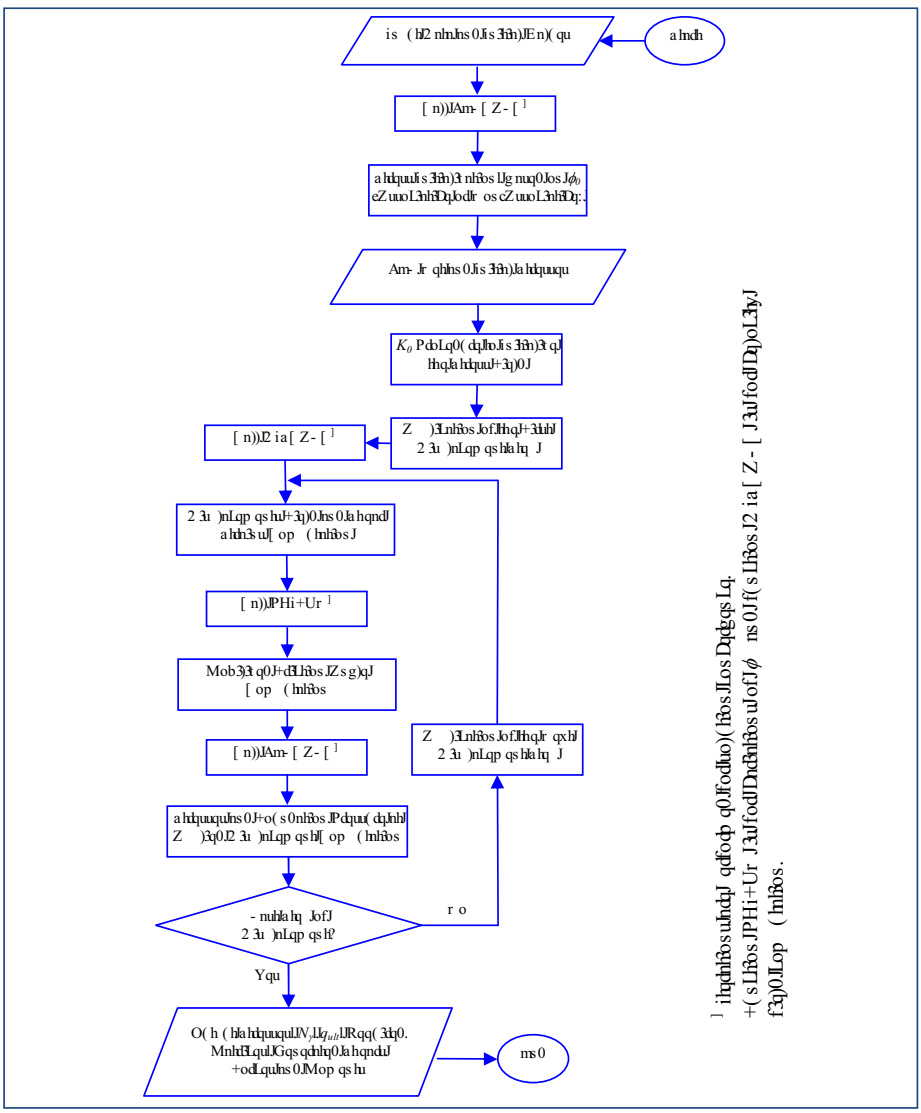

Fig. 14. Mohr's circle of a) stresses and b) strains; to find σ_{sp} and γ_{sp}